Mesoscopic Impurities Expose a Nucleation-Limited Regime of Crystal Growth

Mike Sleutel,[1,*] James F. Lutsko,[2] Dominique Maes,[1] and Alexander E. S. Van Driessche[1]
[1]*Structural Biology Brussels, Vrije Universiteit Brussel, Pleinlaan 2, 1050 Brussels, Belgium*
[2]*Center for Nonlinear Phenomena and Complex Systems, Code Postal 231, Université Libre de Bruxelles, Boulevard du Triomphe, 1050 Brussels, Belgium*
(Received 19 February 2015; published 15 June 2015)

Nanoscale self-assembly is naturally subject to impediments at the nanoscale. The recently developed ability to follow processes at the molecular level forces us to resolve older, coarse-grained concepts in terms of their molecular mechanisms. In this Letter, we highlight one such example. We present evidence based on experimental and simulation data that one of the cornerstones of crystal growth theory, the Cabrera-Vermilyea model of step advancement in the presence of impurities, is based on incomplete physics. We demonstrate that the piercing of an impurity fence by elementary steps is not solely determined by the Gibbs-Thomson effect, as assumed by Cabrera-Vermilyea. Our data show that for conditions leading up to growth cessation, step retardation is dominated by the formation of critically sized fluctuations. The growth recovery of steps is counter to what is typically assumed, not instantaneous. Our observations on mesoscopic impurities for lysozyme expose a nucleation-dominated regime of growth that has not been hitherto considered, where the system alternates between zero and near-pure velocity. The time spent by the system in arrest is the nucleation induction time required for the step to amass a supercritical fluctuation that pierces the impurity fence.

DOI: 10.1103/PhysRevLett.114.245501 PACS numbers: 81.10.Dn, 68.37.Ps, 82.20.Wt

Nucleation and growth are considered two separate stages of all first order phase transitions. The delineation between the two is the transition from a stochastic regime driven by fluctuations to a deterministic regime governed by thermodynamics. As a consequence of the high activation barrier that is usually associated with the nucleation process, most crystalline nuclei are formed at relatively high supersaturations [1]. During the growth stage that ensues, supersaturation is gradually lowered until equilibrium is reached, exposing a number of other activation barriers in the process. One well-known example is the barrier for 2D nucleation on the flat faces that make up the crystal habit after the disappearance of kinked and stepped faces [2]. At sufficiently low supersaturation, the formation of new layers by the condensation of admolecules into crystalline islands becomes the rate-limiting step of crystal growth.

Crystal growth eventually arrests by one of two means: (i) by depletion of growth units from the surrounding liquid until the supersaturation $\Delta\mu$ reaches zero or (ii) at some finite $\Delta\mu_d$ by the presence of growth perturbing species distinct from the constituent crystal units, i.e., *impurities*. This impurity induced nonzero value of $\Delta\mu$ where the crystal growth rate is zero defines the width of the so-called *dead zone* [3]. Such a dead zone occurs for a specific class of impurities, namely, those that are firmly adsorbed onto the surface with (near-) infinite residence times (Dynamic residues with finite residence times can in extreme cases lead to kinetic arrest, but only at very high concentrations.) The moments leading up to this growth cessation event have been the subject of intense study [4–11] and are thought to be well understood. The first theoretical description was developed as early as 1958 by Cabrera and Vermilyea (CV) [3], whose core views on the subject still persist today. The CV model for step pinning states that the step velocity is zero below the dead zone supersaturation, and some finite value v above $\Delta\mu_d$.

The important point for our purposes is that growth is predicted to instantaneously reinitialize once $\Delta\mu > \Delta\mu_d$. We stress that CV only considered average velocities based on a mesoscopic model of the steps—a nuance that is typically overlooked. In fact, this was pointed out by the authors themselves in their seminal paper on the subject. In reality, steps do not display the smooth curvatures as assumed in their simplified model, but rather are discrete, atomistic objects subject to fluctuations. This was already realized by Frank [12] and explored further by van Enckevort and van den Berg [9] and more recently by Ranganathan and Weeks who developed a coarse grained terrace-step-kink model to study impurity induced step bunching [10,11].

In this contribution we focus on isolated elementary steps in the classic CV scenario through experimental means and by the use of kinetic Monte Carlo (KMC) simulations. We focus on the early stages of growth recovery at $\Delta\mu = \Delta\mu_d + \delta$ with δ small compared to typical bond energies ϵ. As a case study we follow the impurity-induced growth cessation of an impure ($\leq$95% purity) commercial preparation of hen egg white lysozyme supplied by Sigma-Aldrich. Previously, we demonstrated that Sigma lysozyme displays elementary step kinetics that are not compatible with the predictions made by CV [13].

The optical technique we employed to measure the mean growth rate had only a limited lateral resolution and was therefore blind to the presence of surface bound impurities and the effects they have on local step structure. We identified the supersaturation at which growth cessation starts to occur to be $\beta\Delta\mu = \ln(40/37.5) = 0.065$ with β the inverse temperature. To probe the still-unknown mechanism of this phenomenon [13,14], we revisit the Sigma lysozyme system using atomic force microscopy at conditions close to kinetic arrest. *In situ* atomic force microscopy reveals that the molecular impurities in the liquid self-aggregate into mesoscopic particles that have a high affinity for the (110) face of tetragonal lysozyme crystals (see Supplemental Material [15], Fig. 1). Two types of impurities can be discerned: linear fibrils [Supplemental Material [15], Figs. 1(b) and 1(c)] and amorphous clusters [Supplemental Material [15], Fig. 1(d)]. The adsorbed fibrils are mostly aligned with the $\langle 001 \rangle$ direction [Supplemental Material [15], Fig. 1(e)] suggesting that the interaction with the crystal surface is highly specific. Given that such structures are not observed when using highly purified lysozyme solutions, they must be the result of a molecular aggregation process in the liquid in which the impurity species play a crucial role. The strong impurity-crystal interaction (as inferred from the long impurity residence time on the surface) gives rise to a high density network of linear impurity chains. The atypical anisotropic structure and mesoscopic dimensions of the impurities renders the prevailing model of the impurity fence (randomly dispersed atomic impurities) inapplicable for this case. Rather, the maze of impurities creates a scenario that is more reminiscent of percolation theory and is therefore out of the scope of conventional impurity models.

The impurity effect is maximal (see Supplemental Material [15], Fig. 2) in the $\langle 110 \rangle$ direction where the contact area between the aligned fibrils and steps is maximal. The impurities create *roadblocks* where the local step velocity is effectively zero (Fig. 1). After an induction time of minutes, protuberances are formed by step segments that suddenly burst through the impurity blockade. The local step velocity jumps from 0 nm/s to 2.5 nm/s only to drop back to 0 nm/s when another fibril is encountered. The system effectively cycles through discrete stages of cessation and growth, averaging out to a rate of growth of the entire step front of 0.7 nm/s. We remark that the rapidly emerging terraces that are formed during the breakthrough event of formerly halted step segments are relatively devoid of impurities. This suggests that the equilibrium surface impurity density is not yet reached locally and that kinetic adsorption factors should be taken into account. These kinetic factors will become increasingly relevant for higher supersaturation values where the terrace exposure times become smaller. Also, impurities can persist on the surface even after step fronts have passed (see Supporting Movie 1, [15]). Single steps therefore do not have the cleansing effect that is typically assumed in crystal growth models, i.e., they do not sweep away (all) the impurities (either by incorporation or rejection) from the surface.

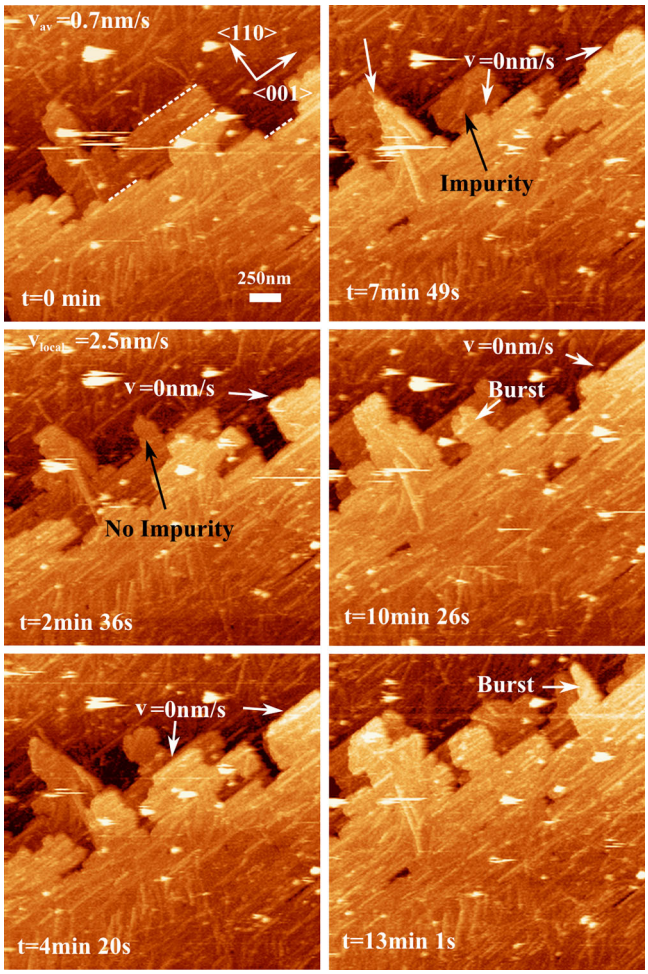

FIG. 1 (color online). Structural evolution of two elementary lysozyme steps growing in the $\langle 110 \rangle$ direction: the dashed white lines at $t = 0$ min indicate step segments where the local step velocity is effectively zero due to blockage by fibrils. After an induction time of minutes, fingers are formed as a consequence of a rapid burst through the impurity blockade. The regained advancement is hampered until the next fibril is reached. The system cycles through $v_{\mathrm{step}} > 0$ and $v_{\mathrm{step}} = 0$. The *fresh* terraces created by the formation of fingers, are relatively devoid of impurities. Gradual impurity binding is observed over the course of the successive frames.

In order to advance through the impurity blockade, steps need to squeeze through slits (with characteristic length Δ) that exist in between parallel impurity chains. Growth cessation criteria predict that steps fail to break through such an obstacle when Δ is smaller than or equal to a critical value [18]. For larger Δ, the steps are expected to breach the slit and continue until the next obstacle is reached. Our data shows that this is not an instantaneous event. When a step encounters a "wall of impurities," there

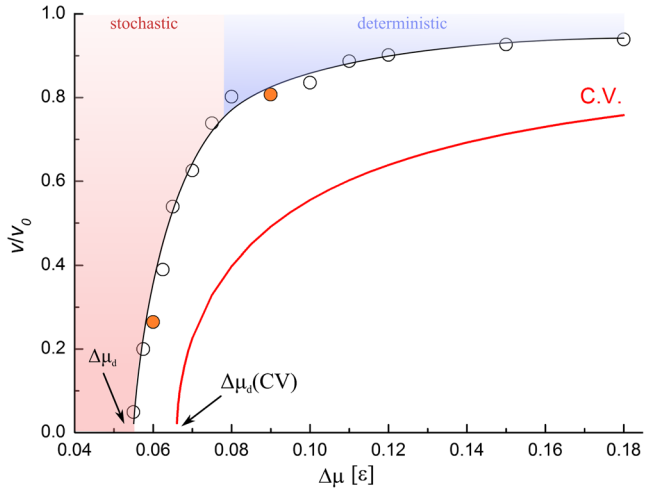

FIG. 2 (color online). Supersaturation dependence of the ratio of the impure growth rate v and the growth rate v_0 of the pure system (circles; black line is a guide for the eye). Red line shows the predicted CV dependence using empirically determined critical radii. Colored data points correspond to the simulations in Fig. 3.

is an initial period during which the mean step velocity is zero, after which a rapid burst in step advancement is observed. The presence of an induction time suggests that the breakthrough moment is governed by a nucleation event. When a local opening of near-critical dimensions of the impurity grid is encountered, the step needs to create a protuberance of adequate size before growth resumes. Such structures, due to their large circumference to surface ratio, are plagued by a high free energy cost of formation. For small structures, the cost of creating the relatively large number of dangling bonds at the periphery dominates the gains of creating satisfied bonds within the center. Given that the crossing of the associated nucleation barrier is driven solely by thermal fluctuations, there is a nonzero waiting time during which the mean growth rate of the step is effectively zero followed by a sudden burst—as is observed in experiment. To get a quantitative understanding of this process, we performed KMC simulations for a similar, albeit, simplified scenario.

Our starting configuration is a flat terrace with a central column of impurities that has a slit of impurity vacancies at its center (see Supplemental Material [15], Fig. 3). For $\Delta\mu > 0$, steps move from left to right in the Supplemental Material [15], Fig. 3 and need to squeeze through the central impurity blockade. We monitored the evolution of the total mass of the system for a broad supersaturation range, keeping the dimension Δ of the central passage constant. The average change in mass over the total simulation time $\langle dM/dt \rangle$ is a good proxy for the step velocity v. This rate is then normalized by the value v_0 obtained for the pure case and plotted as a function of $\Delta\mu$ in Fig. 2. For comparison, we also plot the kinetic recovery that is predicted by the CV step pinning model using

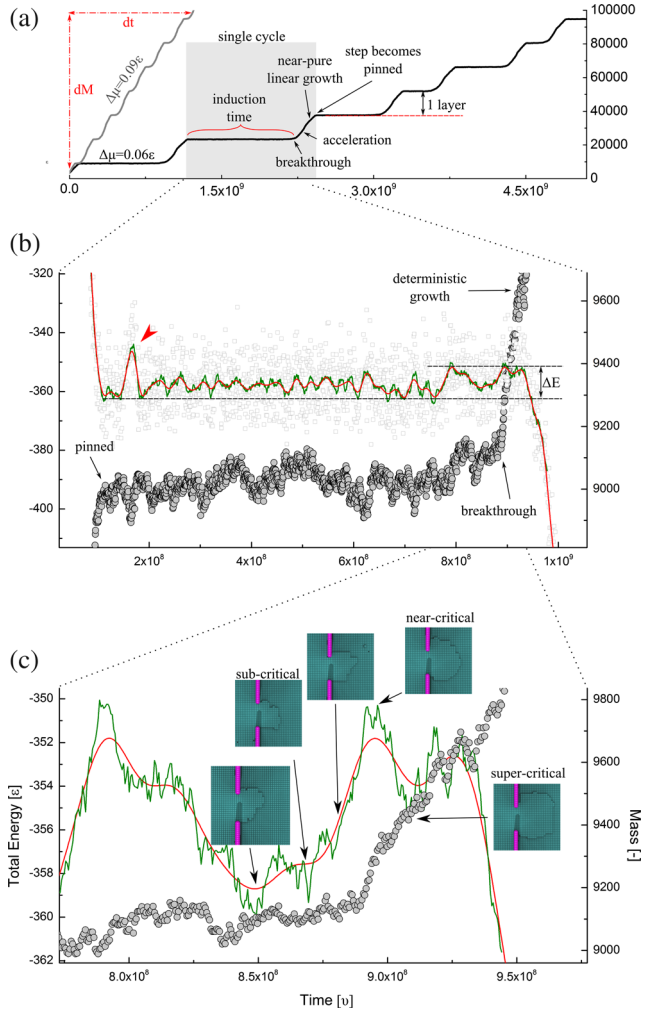

FIG. 3 (color online). (a) Total mass within the simulation cell as a function of time: each cycle starts out in an arrested state during which the mass fluctuates around a constant value. After some induction time, a breakthrough occurs that allows the step to pierce through the impurity blockade. It subsequently accelerates and quickly reaches (near) pure velocity (linear growth) only to become pinned again when the next column of impurities is reached. (b) Total mass (grey circles) and energy (open squares) of a single growth cycle. The green and red lines are smoothed traces of the energy using Savitzky-Golay and Fast Fourier Transform filters, respectively, with a 20-point sliding window. (c) Simulation snapshots and close-ups of the mass and energy evolution close to the breakthrough: the sudden increase of mass coincides with a crossing of a local maximum in energy followed by steady growth during which the energy decreases consistently.

empirically determined r_c values. The discrepancy between the dead zone supersaturation of both cases [$\Delta\mu_d$ and $\Delta\mu_d$ (CV)] has been discussed at length in Lutsko *et al* [18]. Here we are interested in the kinetic response of the system for $\Delta\mu > \Delta\mu_d$. The CV trace clearly shows a weaker dependence than the v/v_0 trace obtained from simulation.

Probing for the origins of this stronger supersaturation dependence, we looked at the temporal evolution of the

total mass and energy of the system in more detail. The mass trace shown in Fig. 3(a) is representative of higher supersaturation values and is in complete accordance with the classical CV picture. It highlights the stepwise, cyclic nature of the process. As a planar step front arrives at the impurity blockade it needs to squeeze through the central impurity-free slit, and decelerates as a consequence of the Gibbs-Thomson effect, rapidly regaining its near-pure velocity as the blockade is passed. The important point here is that the temporal length of each cycle is roughly constant and the step velocity never reaches zero.

This regularity is lost for conditions closer to $\Delta\mu_d$, see for example the $\Delta\mu = 0.06\epsilon$ trace in Fig. 3(a). The time spent by the system at constant mass is considerably longer and varies from cycle to cycle. The enlargement in Fig. 3(b) shows the mass and energy fluctuations during a single obstruction stage. After a given induction time, a breakthrough event occurs that is characterized by a rapid increase (decrease) of mass (energy). The further enlargement in Fig. 3(c) demonstrates that the sudden increase of mass coincides with a crossing of a local maximum in energy followed by a stage of steady growth during which the energy decreases consistently. Essentially, the step fragment needs to accumulate a critical mass defined by a critical energy in order to overcome the impurity obstruction. The process is driven solely by fluctuations and can therefore be regarded as a *nucleation event* that is characterized by a nucleation activation barrier ΔE. We also include the simulation snapshots of the moments leading up to the step-breakthrough [Fig. 3(c)]: in line with nucleation terminology we divide the step fragments in groups of sub-, near- and super-critical mass. It is interesting to note that subcritical step fragments close to the actual breakthrough moment change very little in mass, but do correspond to gradual increases in energy.

Extracting meaningful estimates of the activation barrier is less trivial than one would initially assume. The finger morphology and the nucleation barrier that must be overcome are closely related. The critical size depends on the shape of the finger since this determines the length of the boundary of the finger (for fixed total mass) and this, in turn, determines the contribution of line tension to the total free energy. Note for instance the red arrowhead in Fig. 3(b): it highlights a local maximum in energy ($> \Delta E$) that is not correlated to a significant change in mass. This demonstrates that the system cannot be described by a single order parameter, local step structure needs to be taken into account as well. The *nonproductive* fluctuation around $t = 1.8 \times 10^8 \nu^{-1}$ (with ν the KMC attempt frequency) is a reorganization to a step morphology that is characterized by a larger critical mass (that is not reached) and therefore does not lead to a breakthrough.

Reverting back to Fig. 2, we can now rationalize the increased supersaturation dependence with respect to CV. For high supersaturation, step deceleration is dominated by the Gibbs-Thomson effect [19,20] induced by the local step curvature that is created as the step squeezes through the blockade (deterministic regime). For lower supersaturation, the deceleration is predominantly caused by the accumulated induction time spent by the system in arrest leading to the observed stop-and-go dynamics (stochastic regime). As supersaturation decreases, the induction time is expected to increase exponentially, as is the reduction in growth rate. Effectively, the nucleation of supercritical step protuberances becomes the rate-limiting step, and crystal growth as a whole becomes nucleation limited thus qualitatively reproducing the experimental observations. Because nucleation in this case is effectively driven by step meandering, it will be tightly related to the density of kinks of the pinned step segment. If the static mean excursion of the step segment is supercritical, steps will be relatively unencumbered by the impurity stoppers. If the supersaturation decreases, the time during which the steps remain pinned will depend on the height of the activation barrier (which sets the amplitude of the required step fluctuation) and the frequency of nucleation attempts (which is governed by the rate of terrace width equilibration [21]), both of which depend on the kink density.

Our data demonstrate that step advancement close to the cessation condition becomes an activated process where "nucleation" of step protuberances that pierce the grid of impurities becomes the rate-limiting step. This nucleation dominated regime of step advancement exposes an activation barrier that poses serious restrictions to the advancement of steps which has not been hitherto considered. In many cases, crystallographic impurities are comparable in size to the main building blocks of the growing crystal. The mesoscopic impurities we observe can be 2 to 3 orders of magnitude longer in length than a single lysozyme molecule. There are numerous examples of crystallization systems that are perturbed by linear impurities, leading to strong nonlinear step kinetics. Notable examples are peptide-biomineral systems (calcite [22], apatite [23], calcium oxalate monohydrate [24,25]) and anti-freeze polymer, and ice [26,27]. In fact, stop-and-go dynamics were also observed by Weaver *et al.* for calcium oxalate monohydrate [25]. Although they implemented a two-step impurity adsorption model to rationalize the bistable growth, the similarity with the case presented here is remarkable.

We stress that the stochastic growth regime presented here is a general concept that applies to all types of surface bound impurities, regardless of their size. To illustrate this point, we end with a qualitative simulation, identical to the one in Fig. 3 but with impurities similar in size (3×1) to the growth species (see Supplemental Material [15], Fig. 4). As expected, there is a clear induction time associated with the passing of each column of equidistant spaced impurities. The small difference with larger impurities is that

adjoining step segments can interact and cross the impurities in a cooperative manner. Our observations for Sigma lysozyme differ from existing models on two essential points: (i) the cleansing assumption of the Frank model does not hold, and (ii) the anisotropic shape of the impurities leads to step orientation dependent effects. These features need to be taken into account in the future development of more general impurity models.

The work of M. S., J. F. L., D. M., and A. E. S. V. D. is supported in part by the European Space Agency under Contract No. ESA AO-2004-070 and the FWO Grant No. 1523115N.

*Corresponding author.
msleutel@vub.ac.be

[1] A. A. Chernov, J. Struct. Biol. **142**, 3 (2003).
[2] D. Kashchiev, *Nucleation—Basic Theory with Applications* (Butterworth-Heinemann, London, 2000).
[3] N. Cabrera and D. A. Vermilyea, in *Growth and Perfection of Crystals*, edited by R. Doremus, B. Roperts, and D. Turnbull (Wiley, New York, 1958), pp. 393–410.
[4] N. Kubota and J. Mullin, J. Cryst. Growth **152**, 203 (1995).
[5] M. L. Weaver, S. R. Qiu, R. W. Friddle, W. H. Casey, and J. J. De Yoreo, Cryst. Growth Des. **10**, 2954 (2010).
[6] S. Y. Potapenko, J. Cryst. Growth **133**, 147 (1993).
[7] S. Y. Potapenko, J. Cryst. Growth **133**, 141 (1993).
[8] J. J. De Yoreo, L. A. Zepeda-Ruiz, R. W. Friddle, S. R. Qiu, L. E. Wasylenki, A. A. Chernov, G. H. Gilmer, and P. M. Dove, Cryst. Growth Des. **9**, 5135 (2009).
[9] W. J. P. van Enckevort and A. C. J. F. van den Berg, J. Cryst. Growth **183**, 441 (1998).
[10] M. Ranganathan and J. D. Weeks, Phys. Rev. Lett. **110**, 055503 (2013).
[11] M. Ranganathan and J. D. Weeks, J. Cryst. Growth **393**, 35 (2014).
[12] F. C. Frank, in *Growth and Perfection of Crystals*, edited by R. Doremus, B. Roperts, and D. Turnbull (Wiley, New York, 1958), pp. 411–419.
[13] M. Sleutel and A. E. S. Van Driessche, Cryst. Growth Des. **13**, 688 (2013).
[14] M. Sleutel, G. Sazaki, and A. E. S. Van Driessche, Cryst. Growth Des. **12**, 2367 (2012).
[15] See Supplemental Material at http://link.aps.org/supplemental/10.1103/PhysRevLett.114.245501 for details on Methods section and 3 Supplementary Figures, which includes Refs. [16,17].
[16] Y. Saito, *Statistical Physics of Crystal Growth* (World Scientific, Singapore, 1996).
[17] I. Horcas, R. Fernández, J. M. Gómez-Rodríguez, J. Colchero, J. Gómez-Herrero, and A. M. Baro, Rev. Sci. Instrum. **78**, 013705 (2007).
[18] J. F. Lutsko, N. González-Segredo, M. A. Durán-Olivencia, D. Maes, A. E. S. Van Driessche, and M. Sleutel, Cryst. Growth Des. **14**, 6129 (2014).
[19] J. W. Gibbs, Trans. Conn. Acad. Arts Sci. **3**, 108 (1876).
[20] J. W. Gibbs, Trans. Conn. Acad. Arts Sci. **16**, 343 (1878).
[21] N. C. Bartelt, J. L. Goldberg, T. L. Einstein, and E. D. Williams, Surf. Sci. **273**, 252 (1992).
[22] S. Elhadj, E. A. Salter, A. Wierzbicki, J. J. De Yoreo, N. Han, and P. M. Dove, Cryst. Growth Des. **6**, 197 (2006).
[23] A. George and A. Veis, Chem. Rev. **108**, 4670 (2008).
[24] R. W. Friddle, M. L. Weaver, S. R. Qiu, A. Wierzbicki, W. H. Casey, and J. J. De Yoreo, Proc. Natl. Acad. Sci. U.S.A. **107**, 11 (2010).
[25] K. R. Cho, E. A. Salter, J. J. De Yoreo, A. Wierzbicki, S. Elhadj, Y. Huang, and S. R. Qiu, Cryst. Eng. Comm. **15**, 54 (2013).
[26] M. I. Gibson, Polym. Chem. **1**, 1141 (2010).
[27] M. L. Huang, D. Ehre, Q. Jiang, C. Hu, K. Kirshenbaum, and M. D. Ward, Proc. Natl. Acad. Sci. U.S.A. **109**, 19922 (2012).